Low-Damping Spin-Wave Transmission in YIG/Pt-Interfaced Structures

Rostyslav O. Serha, Dmytro A. Bozhko, Milan Agrawal, Roman V. Verba, Mikhail Kostylev, Vitaliy I. Vasyuchka, Burkard Hillebrands,* and Alexander A. Serga*

Magnetic heterostructures consisting of single-crystal yttrium iron garnet (YIG) films coated with platinum are widely used in spin-wave experiments related to spintronic phenomena such as the spin-transfer-torque, spin-Hall, and spin-Seebeck effects. However, spin waves in YIG/Pt bilayers experience much stronger attenuation than in bare YIG films. For micrometer-thick YIG films, this effect is caused by microwave eddy currents in the Pt layer. This paper reports that by employing an excitation configuration in which the YIG film faces the metal plate of the microstrip antenna structure, the eddy currents in Pt are shunted and the transmission of the Damon–Eschbach surface spin wave is greatly improved. The reduction in spin-wave attenuation persists even when the Pt coating is separated from the ground plate by a thin dielectric layer. This makes the proposed excitation configuration suitable for injection of an electric current into the Pt layer and thus for application in spintronics devices. The theoretical analysis carried out within the framework of the electrodynamic approach reveals how the platinum nanolayer and the nearby highly conductive metal plate affect the group velocity and the lifetime of the Damon–Eshbach surface wave and how these two wavelength-dependent quantities determine the transmission characteristics of the spin-wave device.

1. Introduction

Magnonics and magnon spintronics address the transfer and processing of information using spin waves and their quanta, magnons.[1–6] One main challenge for this field is the finite lifetime of magnons even in low-damping magnetic materials such as single crystal yttrium iron garnet (YIG, $Y_3Fe_5O_{12}$) films.[7] A possible way to overcome this issue is by compensating spin-wave damping via transfer of a spin momentum from an adjacent non-magnetic metal layer with high spin-orbit interaction to a magnetic medium by using a spin-polarized electron current.[8,9] The decrease in the damping of spin waves propagating in a YIG film covered with a current-conducting Pt film has already been reported.[10,11] However, the base (i.e., zero-current) spin-wave attenuation in the investigated structures is unacceptably high for practical applications ($\simeq$35 dB in ref. [10]).

Originally, the source of this attenuation was exclusively linked to the process of spin-momentum transfer back to a non-magnetic metal layer that plays the role of a spin sink.[12] In ref. [13], we have shown experimentally and theoretically that ohmic losses of eddy currents, which are induced in the Pt layer by the precessing magnetization vector, deliver a strong contribution to the ferromagnetic resonance linewidth in micrometer-thick YIG films. Furthermore, we were able to successfully reduce this damping by shunting the eddy currents with a highly conducting metal plate.[13] The contributions of spin pumping, which affect the Gilbert damping and hence the attenuation of spin waves, can be neglected in this case since the thickness of the YIG layer was large. These experiments were performed using standing backward volume spin waves in laterally confined YIG-film samples. The magnetization dynamics in the samples were

R. O. Serha, D. A. Bozhko, M. Agrawal, V. I. Vasyuchka,
B. Hillebrands, A. A. Serga
Fachbereich Physik and Landesforschungszentrum OPTIMAS
Technische Universität Kaiserslautern
67663 Kaiserslautern, Germany
E-mail: hilleb@physik.uni-kl.de; serga@physik.uni-kl.de

R. O. Serha
Faculty of Physics
University of Vienna
Vienna 1090, Austria

D. A. Bozhko
Department of Physics and Energy Science
University of Colorado Colorado Springs
Colorado Springs, CO 80918, USA

R. V. Verba
Department of Physics of Meso- and Nanocrystalline
Magnetic Structures
Institute of Magnetism
Kyiv 03142, Ukraine

M. Kostylev
Department of Physics and Astrophysics
University of Western Australia
Crawley, WA 6009, Australia

ADVANCED
SCIENCE NEWS
www.advancedsciencenews.com

ADVANCED
MATERIALS
INTERFACES
www.advmatinterfaces.de

driven by a spatially uniform microwave magnetic field of a rectangular waveguide.

At the same time, many practical applications require the ability to control the attenuation of travelling spin waves in combination with a good spin-wave excitation efficiency and within a broad frequency band.[14–16]

Recently, it was shown that the additional attenuation of a travelling spin wave in in-plane magnetized YIG-metal bilayers is also caused by eddy currents.[14,16]

Here, we present a method to overcome the additional attenuation of a traveling surface spin wave (the Damon–Eschbach magnon mode, DE) that propagates perpendicular to the direction of sample magnetization in an in-plane magnetized YIG film coated with Pt. We utilize the standard microstrip structure[10] for the excitation and detection of DE waves but flip the orientation of the magnetic film with respect to the microstrip antennas and the ground plane (see **Figure 1**). Placing the Pt layer of the bilayer structure near the highly conducting ground plate suppresses the excitation of eddy currents in the much less conducting platinum layer.[13,17] This ensures a large increase (up to 1000 times) in the transmission of the long-wavelength DE wave through a two-port magnonic device. The experimental findings are in good agreement with solutions of the corresponding electrodynamical problem. The theoretical calculations reveal a dependence of the magnon lifetime on the spin-wave wavelength and show that an increase in the group velocity of the wave due to the proximity of the highly conducting metal surface plays an important role in this process.

2. Results and Discussions

2.1. Experiment

The experiments were performed using 2 mm-wide and 15 mm-long spin-wave waveguides prepared from a 6.7 µm-thick YIG film. The film was grown with the liquid phase epitaxy method on a 500 µm-thick gadolinium gallium garnet (GGG) substrate. A 10 nm-thick Pt layer was deposited on top of the YIG surface.
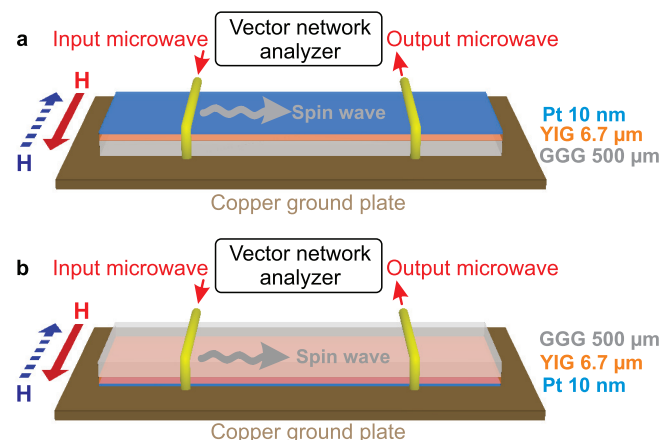

Figure 1. Sketch of the experimental setup. a) Conventional spin-wave excitation configuration—a YIG-Pt bilayer is placed near the microstrip antennas. b) Inverted spin-wave excitation configuration—the YIG-Pt bilayer is close to the ground plate of the microstrip structure.

Spin waves were emitted and received by two short-circuited gold-wire antennas of 50 µm diameter placed 7.6 mm apart from each other (see Figure 1). The spin-wave propagation was studied in a frequency band from 6.2 to 6.5 GHz using a vector network analyzer Anritsu MS46322A. A relatively small level of the applied microwave power of 0.5 mW was chosen to prevent development of nonlinear effects for the propagating spin waves. An external bias magnetic field $\mu_0 H = 160$ mT was applied in the YIG film plane perpendicularly to the spin-wave propagation direction. In this way, the Damon–Eshbach configuration was implemented.[18]

2.1.1. Conventional Excitation Configuration

The reference experiment was performed in a conventional excitation configuration (as in ref. [10]), when a YIG film sits directly under the antennas (see Figure 1a and sketches of the experimental geometry in **Figure 2**). In the case of a bare YIG film—that is, without Pt coating (Figure 2a), the DE spin wave, which is localized near the YIG surface, on which the antennas are placed (see the sketch of the spin-wave amplitude distribution over the YIG film thickness in Figure 2a), possesses relatively low transmission losses—of around 10 dB for the maximum of the transmission band (at 6.42 GHz). The DE
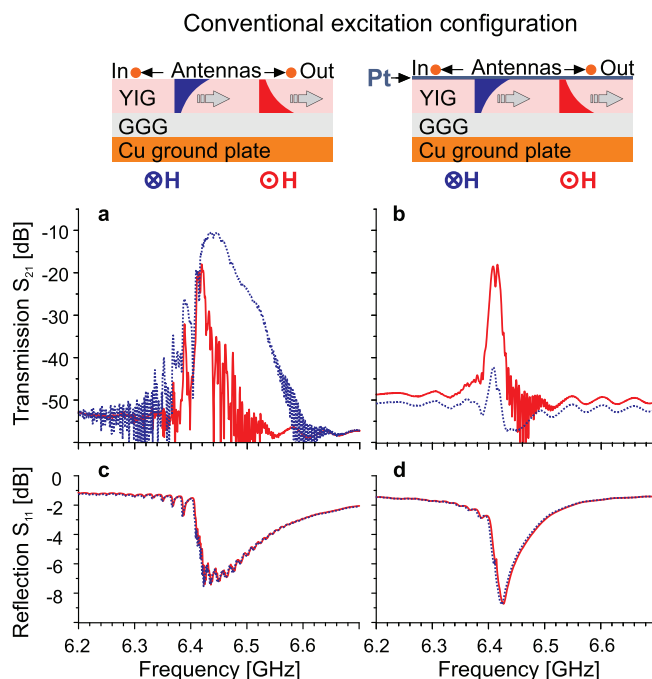

Figure 2. Conventional excitation configuration. A YIG film is positioned directly under the antennas. The localization of a Damon–Eshbach wave depends on the direction of the bias magnetic field H (see red and blue profiles within the YIG layer on the sketches of the experimental geometry). Dotted/blue lines correspond to the bias magnetic field pointing into the drawing plane. Solid/red lines correspond to the bias magnetic field pointing out of the drawing plane. a,b) Transmission (S_{21}) characteristic of the bare YIG waveguide and of the YIG waveguide covered with a 10 nm-thick Pt layer, respectively. c,d) Excitation efficiency of the input antenna (S_{11}) for the bare YIG waveguide and for the YIG waveguide covered with the 10 nm-thick Pt layer, respectively.

**ADVANCED
SCIENCE NEWS**

www.advancedsciencenews.com

**ADVANCED
MATERIALS
INTERFACES**

www.advmatinterfaces.de

wave localized at the opposite film surface shows a one order of magnitude weaker transmission. This well-known effect relates to the nonreciprocal excitation of the DE wave, whose efficiency depends on the relative orientation of the bias magnetic field H with respect to the spin-wave propagation direction.[7,19–22] In spite of the pronounced difference in the transmission characteristics, the efficiencies of spin-wave excitation, which scale with the inverse of the microwave reflection from the input antenna S_{11}, are identical for the two opposite orientations of the bias magnetic field (see Figure 2c). That is because the input antenna always emits spin waves in opposite directions simultaneously and both waves contribute to the measured S_{11}. The nonreciprocity in the spin-wave transmission appears because only the wave emitted toward the output antenna contributes to the transmission characteristic S_{21}.

In the case of the Pt-covered YIG film, the excitation efficiency remains almost the same as for the reference single-layer YIG waveguide (compare Figures 2c,d) but the transmission of the DE wave localized near the Pt layer is strongly suppressed (see the dashed blue curve in Figure 2b). This suppression is associated with ohmic losses of the eddy currents excited in the low-conductance Pt layer by stray fields of the propagating spin wave.[13,16]

2.1.2. Inverted Excitation Configuration

In the second stage of our studies, the YIG film was facing the ground plate (see Figures 1b and **3**). If the Pt film is in a direct electric contact with the bulk copper plate, the eddy currents will mostly flow in the low-resistance ground plate. Hence, no additional ohmic losses due to microwave currents in Pt are expected.

The spin-wave excitation efficiencies shown in Figure 3c,d for the bare and Pt-covered YIG waveguides are close to those obtained in the conventional excitation configuration (compare to Figure 2c,d). At the same time, from Figure 3a,b, one sees that the wave localized at the Pt layer now experiences no excessive damping. It is now characterized by the same level of transmission losses as the wave in the bare YIG film. This fact confirms a significant contribution of the spin-wave-induced eddy currents to the damping of the surface spin waves in Pt-YIG bilayers.

It should be noted that in the proposed inverted excitation configuration, spin waves are excited mostly by microwave currents flowing in the ground plate rather than by currents flowing through the microstrip antenna. The latter is separated from the YIG film by a thick GGG substrate; therefore, the current in it cannot contribute significantly to the wave excitation process. This decreases the overall excitation efficiency of short-wavelength spin waves. It happens because the microwave currents in the extended ground plate are not confined by the conductor geometry as strongly as in the microstrip antenna and can spread over a larger area in the plate plane.

Simultaneously, the change in the electrodynamic boundary conditions due to placing the highly conducting plate near the surface of the YIG film[23] makes the slope of the DE dispersion relation steeper. The latter extends the frequency range for a fixed wavelength range of the excited DE waves. In addition, the group velocity of the DE wave increases, which leads to a decrease in its propagation time and, consequently, to a
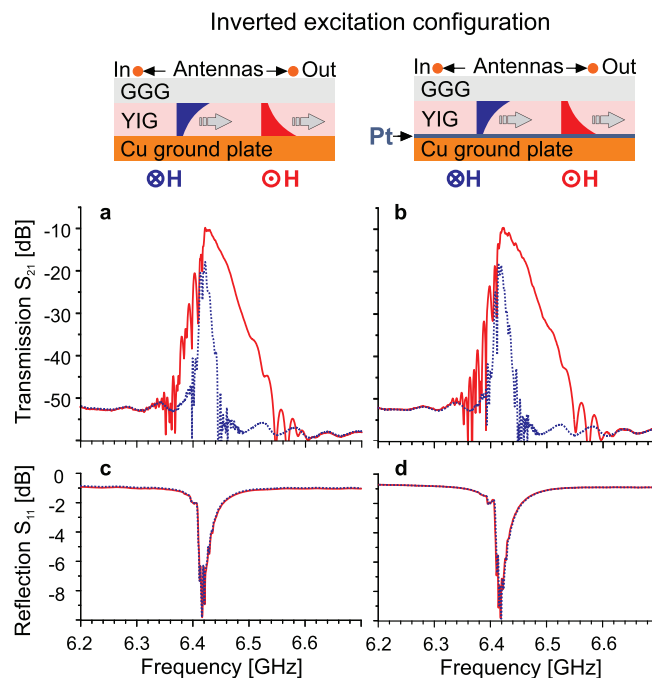

Figure 3. Inverted excitation configuration. The YIG waveguide is positioned directly on top of the copper ground plate. Dotted/blue lines correspond to the bias magnetic field pointing into the drawing plane and solid/red lines correspond to the bias magnetic field pointing out of the drawing plane. a,b) Transmission (S_{21}) characteristics of the bare YIG waveguide and of the YIG waveguide covered with a 10 nm Pt layer, respectively. c,d) Excitation efficiency of the input antenna (S_{11}) for the bare YIG waveguide and for the YIG waveguide covered with the 10 nm-thick Pt layer, respectively. Insets are sketches of localization of the surface spin wave for different directions of the bias magnetic field.

decrease in the transmission losses. As a result, the transmission bandwidth remains sufficiently wide.

2.1.3. Inverted Excitation Configuration with Dielectric Spacer Between Pt Layer and Cu Plate

The described configuration allows surface DE spin waves to propagate over fairly long distances through waveguides made of a YIG film coated with Pt. However, applying a direct electric current to the structure[10,11] or detecting the magnon transport using the constant voltage, which is generated in the Pt layer[24,25] due to the combined action of the spin pumping[26] and the inverse spin Hall effect,[27] is impossible because of the electrical contact between the Pt layer and the ground Cu plate. In order to resolve the issue, we placed a 80 μm-thick polypropylene spacer between the Pt surface and the ground plate (see sketches of the experimental geometry in **Figure 4**). In this case, the minimal transmission losses (Figure 4a,b) remain the same as for the previous measurements (compare Figures 2a and 3a,b), but the transmission bandwidth becomes significantly narrower. In the case of the Pt-covered YIG film, the relative bandwidth reduction is about 14% at −3 dB, 28% at −10 dB, and 32% at −20 dB of the maximal transmission level.

The reason for this bandwidth narrowing is obvious. The dynamic dipole field of a spin wave decays exponentially with
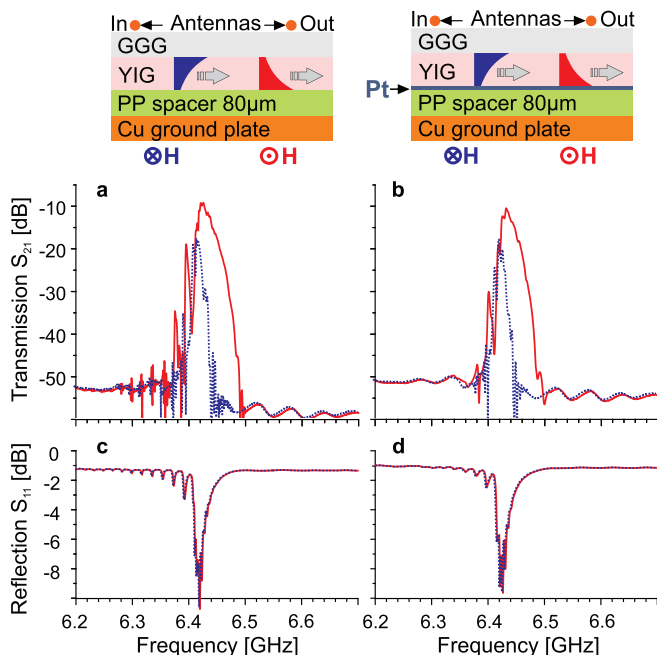
**ADVANCED
SCIENCE NEWS**

www.advancedsciencenews.com

**ADVANCED
MATERIALS
INTERFACES**

www.advmatinterfaces.de

Figure 4. Inverted excitation configuration with dielectric spacer. The YIG waveguide is positioned near the copper ground plate. An additional 80 µm-thick dielectric polypropylene (PP) spacer layer is introduced to electrically decouple the Pt layer from the ground. Dotted/blue lines correspond to the bias magnetic field pointing into the drawing plane. Solid/red lines correspond to the bias magnetic field pointing out of the drawing plane. a,b) Transmission (S_{21}) characteristics of the bare YIG waveguide and of the YIG waveguide covered with a 10 nm-thick Pt layer, respectively. c,d) Excitation efficiency of the input antenna (S_{11}) for the bare YIG waveguide and for the YIG waveguide covered with the 10 nm-thick Pt layer, respectively. Insets are sketches of localization of the surface spin wave for different directions of the bias magnetic field.

the distance d from the film surface. Importantly, the field amplitude decrement equals the spin-wave wavenumber $|k|$ (see Equation (5) in ref. [28]). Accordingly, the range of k-values affected by the presence of the ground plate is $|k|d < 1$. Spin waves with wavenumbers that satisfy this condition feel more strongly the presence of the highly conductive thick ground plate at the distance d than the presence of a thin low-conductance Pt layer in the immediate contact with the YIG surface. This results in a large group velocity and, thus, small transmission losses for the longer-wavelength DE waves. Conversely, for $|k|d \gg 1$, the influence of the ground plate on spin waves is negligible. This leads to larger transmission losses for the shorter-wavelength spin waves due to a smaller group velocity. Then we may expect that with an increase in d, the range of wavenumbers of DE waves with the group velocities affected by the presence of the metal plate becomes smaller. This is the reason why the bandwidth shown in Figure 4 appears narrower than in Figure 3.

2.2. Theory

In order to better understand the experimental results, we performed calculations of the frequencies and lifetime of the propagating surface spin waves in a YIG film located in the vicinity of a highly conducting metal plate. To this end, we solved an electrodynamic problem for the entire layered structure. Similar calculations, but for different geometry of the backward volume magnetostatic waves, were performed in ref. [13].

2.2.1. Theoretical Model

The modeled geometry is as follows. Infinitely extended metallic (Cu and Pt), dielectric and ferrimagnetic layers form a stack in the y direction. The layers are assumed to be continuous in the x–z plane. The bias magnetic field **H** and the static magnetization **M₀** of the YIG layer are parallel to the z axis. In our experiment the sizes of the YIG sample are significantly larger than the exchange length for YIG; therefore, we neglect the exchange interaction. We solve the Maxwell equations accounting for a proper magnetic permeability tensor for the ferromagnetic layer. We assume that the dynamic electric and magnetic fields for all layers have the following form

$$h(\mathbf{r},t), E(\mathbf{r},t) \approx e^{-qy}e^{-ik_x x}e^{i\omega t} \tag{1}$$

A small finite transversal wavenumber k_z of the DE mode in the z direction, which may exist due to a nonuniform profile of static demagnetization fields,[29,30] is neglected (i.e., $k_z = 0$).

Substituting Equation (1) into the Maxwell equations yields relations between components of the electromagnetic field. A general solution for the nonmagnetic layers are expressed as

$$
\begin{aligned}
h_{x,j} &= A_j e^{-q_j y} + B_j e^{q_j y} \\
h_{y,j} &= -\frac{ik_x}{q_j} A_j e^{-q_j y} + \frac{ik_x}{q_j} B_j e^{q_j y} \\
E_{z,j} &= \frac{i\omega\mu_0}{q_j} A_j e^{-q_j y} - \frac{i\omega\mu_0}{q_j} B_j e^{q_j y}
\end{aligned}
\tag{2}
$$

and other components $E_x = E_y = h_z = 0$. This solution corresponds to a transverse electric (TE) electromagnetic wave. One more solution is a transverse magnetic (TM) wave having nonzero components E_x, E_y, and h_z, and all other field components vanishing. This wave does not interact with magnetization oscillations in YIG and is not considered here. In the equations above, index j corresponds to a specific layer ("Cu," "GGG," "Pt," "Air"), and $q_j = \sqrt{k_x^2 - \omega^2\varepsilon_j\varepsilon_0\mu_0}$. For the conductive layers (Pt and Cu), the electric permittivity is $\varepsilon = 1 - i\sigma/(\omega\varepsilon_0)$, where σ is the conductivity. The solution for the ferromagnetic layer reads

$$
\begin{aligned}
h_x &= Ae^{-Qy} + Be^{Qy} \\
h_y &= \xi_- Ae^{-Qy} + \xi_+ Be^{Qy} \\
E_z &= \zeta_- Ae^{-Qy} + \zeta_+ Be^{Qy}
\end{aligned}
\tag{3}
$$

Here, $\xi_\pm = i(k_x\mu \pm q\mu_a)/(k_x\mu_a \pm q\mu)$, $\zeta_\pm = i\omega\mu_0(\mu_a^2 - \mu^2)/(k_x\mu_a \pm q\mu)$, and the "effective wavenumber" is given by $Q^2 = k_x^2 - \omega^2\varepsilon\varepsilon_0\mu_0(\mu^2 - \mu_a^2)/\mu$. The components of the relative magnetic permeability tensor $\hat{\mu}$ for a ferromagnetic medium are given by

$$\mu = \frac{\omega_H(\omega_H + \omega_M) - \omega^2}{\omega_H^2 - \omega^2} \text{ and } \mu_a = \frac{\omega\omega_H}{\omega_H^2 - \omega^2} \tag{4}$$

**ADVANCED
SCIENCE NEWS**

www.advancedsciencenews.com

**ADVANCED
MATERIALS
INTERFACES**

www.advmatinterfaces.de

where $\omega_H = \gamma\mu_0(H + i\Delta H)$, $\omega_M = \gamma\mu_0 M_0$, γ is the gyromagnetic ratio, and ΔH is the ferromagnetic resonance linewidth for an isolated YIG layer (i.e., it accounts for magnetic losses only).

We analyzed the following four structures: i) Cu-GGG-YIG-Air, ii) Cu-GGG-YIG-Pt-Air, iii) Cu-YIG-GGG-Air, and iv) Cu-Pt-YIG-GGG-Air. The first two correspond to the case of conventional and the last two to the inverted excitation configuration. Using the above solutions and requiring continuity of h_x and E_z (the condition for the dynamic magnetic induction b_y is the same as for E_z) at all the boundaries, we obtain a system of equations for coefficients A_j, B_j. Obviously, $B_{Air} = 0$ and $A_{Cu} = 0$, as they describe solutions that diverge at $\pm\infty$ for air and Cu, respectively. The condition of compatibility (vanishing determinant) for this system of linear equations yields a relation between a complex-valued frequency and the DE wave wavenumber $\omega = \omega(k_x)$. The real part of ω is the frequency of the traveling spin wave, and the inversed imaginary part is the corresponding lifetime of surface magnons, $T = 1/\text{Im}[\omega]$, which takes into account the magnetic and electric losses in the whole structure.

In order to find ω, we assumed the following material parameters. The Cu layer and the Pt film have conductivities of $5.96 \times 10^7\,\text{S m}^{-1}$ and $1.3 \times 10^6\,\text{S m}^{-1}$, respectively. The YIG layer, GGG substrate, and semi-infinite air-filled space (denoted as "Air" in Figure 5) are assumed to be dielectrics with zero conductivity. The permittivities of YIG and GGG are $\varepsilon = 15$.[31] Additionally, we set for YIG $M_0 = 140\,\text{kA m}^{-1}$, $\Delta H = 35.8\,\text{A m}^{-1}$ (i.e., 0.45 Oe), $\gamma = 2\pi \times 28\,\text{GHz T}^{-1}$.

The numerical calculation of the complex-valued eigenfrequencies for these material parameters yields dependencies of the angular frequency ω and lifetime T of DE waves on the wavenumber k. These dependencies are shown in **Figure 5** for the four structures mentioned above. By differentiating the dispersion dependencies $\omega(k)$ with respect to k, we calculated the group velocities of the DE waves and then attenuation of their amplitude $A_T = \exp[-l/(v_{gr}T)]$ over a propagation path l of 7.6 mm. The distance l corresponds to the distance between the input and output antennas in our experiment (see Figure 5c,g,k,o). Finally, using the dispersion laws $\omega(k)$ previously found, the A_T versus k dependence was converted into the "transmission characteristics" $A_T(\omega)$ (see Figure 5d,h,l,p). It should be noted that, unlike the experimental transmission characteristics, the calculated transmission characteristics do not include the signal losses during the processes of excitation and reception of spin waves.

2.2.2. Discussion of Theoretical Results

Conventional Configuration Cu-GGG-YIG-Air: For the Cu-GGG-YIG-Air structure, all theoretical dependencies (see Figure 5a–d) are identical for DE waves localized at the YIG film surface facing air and for DE waves localized at the surface of the film facing the GGG substrate (and thus, being separated from the copper plate by the substrate). This is a consequence of the large distance of the YIG film from the metal plate. The slight decrease in the lifetime T for waves with small wavenumbers is a consequence of the fact that T has a following scaling:

$$T = \left(\frac{\partial\omega}{\partial H}\Delta H\right)^{-1},$$ where H is the applied magnetic field and ΔH

is the magnetic loss parameter. In our calculation, ΔH was assumed to be a constant of frequency.

It should be noted that, in contrast to the experiment, there is no non-reciprocity of the theoretical transmission characteristics for these waves. This is due to the fact that such a nonreciprocity is a feature of the process of excitation of the DE spin wave by the magnetic field of the microstrip antenna,[21,22] which was not taken into account in our model.

Conventional Configuration Cu-GGG-YIG-Pt-Air: Placing the 10 nm-thick platinum layer onto the free surface of the YIG film does not significantly change the dispersion characteristics for both waves, but strongly affects their lifetimes. For small wavenumbers, the lifetime of both waves decreases by more than 12 times. As the wavenumber increases, the lifetimes of these waves increase. The increase in T is rather quick for the DE wave localized at the YIG film surface facing the Cu plate. This wave quickly recovers its usual T value determined by the magnetic losses in YIG. Conversely, the increase in the lifetime of the DE wave localized at the Pt-coated surface is significantly slower. Consequently, the transmission characteristics for the latter wave exhibits extraordinary losses (see Figure 5g,h), which correlates well with the results of the experiment shown in Figure 2b.

Inverted Configuration Cu-YIG-GGG-Air: In the inverted configuration, one can see the expected change in the slope of the dispersion characteristic of the DE wave localized at the surface of the YIG film in contact with the massive Cu plate (the red curve in Figure 5i). This causes a sharp increase in the velocity of this wave mentioned in Experimental Section.

The changes in the lifetimes of both waves are more intricate. At $k \simeq 0$, the lifetimes of the DE waves localized at different surfaces of the YIG film are the same and equal to that of the Cu-GGG-YIG-Air structure. As the wavenumber increases, the strength of the wave surface localization increases. This causes a rapid decrease in the lifetime of the DE wave localized at the Cu-YIG interface and a smoother decrease for the DE wave localized at the opposite side of the film. A further increase in the wavenumber leads to an even greater localization of the latter wave at the film side facing away from the metal. This localization reduces the interaction of the DE wave with the metal and leads to an increase in its lifetime. At the same time, the lifetime of the DE wave localized at the film side facing the copper plate monotonically tends to zero in the range of the considered wavenumbers.

Notably, the long lifetime at small wavenumbers and high group velocity of the DE wave localized at the metal-contacting side of the ferrimagnetic film leads to its low propagation losses in the region of small wavenumbers (see the red curve in Figure 5k). Moreover, the steep growth of wave eigenfrequency ω as a function of k leads to a broad frequency band of spin-wave transmission as shown by the red curve in Figure 5l. These theoretical results agree well with the experimental data from Figure 3a for the waves localized at both sides of the YIG film. One important contribution to this good agreement is the fact that for the inverted excitation configuration, there should be no nonreciprocity of excitation of the DE spin wave. However, the measured frequency bands of transmission are
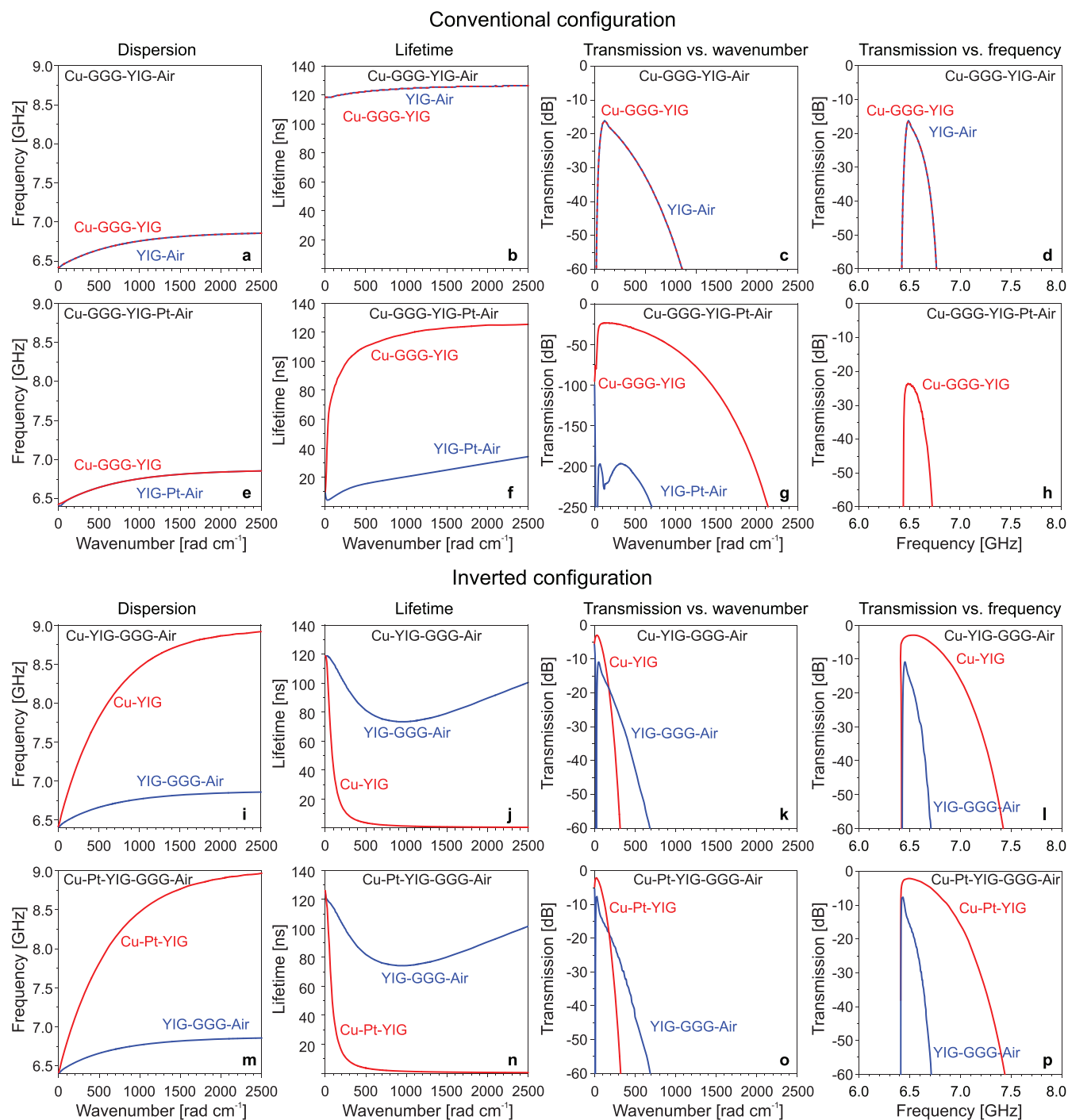
**ADVANCED
SCIENCE NEWS**

www.advancedsciencenews.com

**ADVANCED
MATERIALS
INTERFACES**

www.advmatinterfaces.de

Figure 5. Numerical calculation of dispersion characteristics, lifetimes, and transmission characteristics of the Damon–Eshbach surface spin wave for four layered structures: a–d) conventional configuration Cu-GGG-YIG-Air, e–h) conventional configuration Cu-GGG-YIG-Pt-Air, i–l) inverted configuration Cu-YIG-GGG-Air, and m–p) inverted configuration Cu-Pt-YIG-GGG-Air. The transmission characteristics are calculated as the spin-wave attenuation at a propagation distance of 7.6 mm between antennas and as functions of wavenumber and frequency. The red curves correspond to the case of wave localization at the surface of the YIG film facing the copper ground plate. Blue curves correspond to the case of wave localization at the opposite surface of the YIG film.

much narrower than the theoretical ones because their width is limited by the weak spatial localization of the microwave electric currents in the copper plate.

Inverted Configuration Cu-Pt-YIG-GGG-Air: As Figure 5 shows, placing a thin layer of platinum between the copper plate and the YIG film has almost no effect on the behavior of the DE surface wave because the electrical currents in the platinum layer are shunted by the highly conductive thick metal. This result is also in excellent agreement with the experimental data shown in Figure 3b.

3. Conclusion

In conclusion, we have demonstrated that by using the spin-wave excitation configuration, where a Pt-covered YIG-film waveguide faces the ground plate of a microstrip line structure, it is possible to reduce the excitation eddy currents in the Pt layer that accompany propagation of spin waves in a YIG film capped with the Pt layer. The theoretical analysis demonstrates that despite the presence of ohmic losses caused by eddy currents in the ground plate placed adjacently to the film, the smallness of these losses at small wavenumbers, combined with a significant increase in the group velocity of long-wavelength spin waves, leads to low transmission losses within a reasonably wide frequency band. In particular, our experiments show the same low-loss transmission of a Damon–Eshbach wave in such a structure as for a Damon–Eshbach wave excited by a microstrip antenna placed on the surface of a bare YIG film. Importantly, the inverted configuration does not make technically impossible the application of direct or alternating electric currents to the Pt-layer in spin-transfer-torque experiments or the detection of a spin-Hall-voltage induced in platinum by a propagating spin wave. Thus, the proposed structure has a good potential for use in magnonic and magnon-spintronic devices. We believe that the wavenumber and frequency bandwidth of such devices can be further expanded by stronger spatial localization of microwave currents using specially structured grounding plates or coplanar antennas with metallization between them.

Conflict of Interest

The authors declare no conflict of interest.

Data Availability Statement

The data that support the findings of this study are available from the corresponding author upon reasonable request.

[1] V. V. Kruglyak, S. O. Demokritov, D. Grundler, *J. Phys. D. Appl. Phys.* **2010**, *43*, 264001.

[2] A. V. Chumak, V. I. Vasyuchka, A. A. Serga, B. Hillebrands, *Nat. Phys.* **2015**, *11*, 453.

[3] O. V. Prokopenko, D. A. Bozhko, V. S. Tyberkevych, A. V. Chumak, V. I. Vasyuchka, A. A. Serga, O. Dzyapko, R. V. Verba, A. V. Talalaevskij, D. V. Slobodianiuk, Y. V. Kobljanskyj, V. A. Moiseienko, S. V. Sholom, V. Y. Malyshev, *Ukr. J. Phys.* **2019**, *64*, 888.

[4] A. Barman, G. Gubbiotti, S. Ladak, A. O. Adeyeye, M. Krawczyk, J. Gräfe, C. Adelmann, S. Cotofana, A. Naeemi, V. I. Vasyuchka, B. Hillebrands, H. Yu, D. Grundler, A. V. Sadovnikov, A. A. Grachev, S. E. Sheshukova, J.-Y. Duquesne, M. Marangolo, G. Csaba, W. Porod, V. E. Demidov, S. Urazhdin, S. O. Demokritov, E. Albisetti, D. Petti, R. Bertacco, H. Schultheiss, V. V. Kruglyak, V. D. Poimanov, et al., *J. Phys. Condens. Matter* **2021**, *33*, 413001.

[5] P. Pirro, V. I. Vasyuchka, A. A. Serga, B. Hillebrands, *Nat. Rev. Mater.* **2021**, *6*, 1114.

[6] A. V. Chumak, P. Kabos, M. Wu, C. Abert, C. Adelmann, A. O. Adeyeye, J. Akerman, F. G. Aliev, A. Anane, A. Awad, C. H. Back, A. Barman, G. E. W. Bauer, M. Becherer, E. N. Beginin, V. A. S. V. Bittencourt, Y. M. Blanter, P. Bortolotti, I. Boventer, D. A. Bozhko, S. A. Bunyaev, J. J. Carmiggelt, R. R. Cheenikundil, F. Ciubotaru, S. Cotofana, G. Csaba, O. V. Dobrovolskiy, C. Dubs, M. Elyasi, K. G. Fripp, et al., *IEEE Trans. Magn.* **2022**, *58*, 0800172.

[7] A. A. Serga, A. V. Chumak, B. Hillebrands, *J. Phys. D. Appl. Phys.* **2010**, *43*, 264002.

[8] A. Hamadeh, O. d'Allivy Kelly, C. Hahn, H. Meley, R. Bernard, A. H. Molpeceres, V. V. Naletov, M. Viret, A. Anane, V. Cros, S. O. Demokritov, J. L. Prieto, M. Muñoz, G. de Loubens, O. Klein, *Phys. Rev. Lett.* **2014**, *113*, 197203.

[9] M. Schneider, D. Breitbach, R. O. Serha, Q. Wang, A. A. Serga, A. N. Slavin, V. S. Tiberkevich, B. Heinz, B. Lägel, T. Brächer, C. Dubs, S. Knauer, O. V. Dobrovolskiy, P. Pirro, B. Hillebrands, A. V. Chumak, *Phys. Rev. Lett.* **2021**, *127*, 237203.

[10] Z. Wang, Y. Sun, M. Wu, V. Tiberkevich, A. Slavin, *Phys. Rev. Lett.* **2011**, *107*, 146602.

[11] E. Padrón-Hernández, A. Azevedo, S. M. Rezende, *Appl. Phys. Lett.* **2011**, *99*, 192511.

[12] S. M. Rezende, R. L. Rodríguez-Suárez, A. Azevedo, *Phys. Rev. B* **2013**, *88*, 014404.

[13] S. A. Bunyaev, R. O. Serha, H. Y. Musiienko-Shmarova, A. J. Kreil, P. Frey, D. A. Bozhko, V. I. Vasyuchka, R. V. Verba, M. Kostylev, B. Hillebrands, G. N. Kakazei, A. A. Serga, *Phys. Rev. Appl.* **2020**, *14*, 024094.

[14] I. Bertelli, B. G. Simon, T. Yu, J. Aarts, G. E. Bauer, Y. M. Blanter, T. van der Sar, *Adv. Quantum Technol.* **2021**, *4*, 2100094.

[15] A. Krysztofik, N. Kuznetsov, H. Qin, L. Flajšman, E. Coy, S. van Dijken, *Materials* **2022**, *15*, 2814.

[16] S. Mae, R. Ohshima, E. Shigematsu, Y. Ando, T. Shinjo, M. Shiraishi, *Phys. Rev. B* **2022**, *105*, 104415.

[17] I. S. Maksymov, Z. Zhang, C. Chang, M. Kostylev, *IEEE Magn. Lett.* **2014**, *5*, 3500104.

[18] R. Damon, J. Eshbach, *J. Phys. Chem. Solids* **1961**, *19*, 308.

[19] A. Ganguly, D. Webb, *IEEE Trans. Microwave Theory Tech.* **1975**, *23*, 998.

[20] P. R. Emtage, *J. Appl. Phys.* **1978**, *49*, 4475.

[21] T. Schneider, A. A. Serga, T. Neumann, B. Hillebrands, M. P. Kostylev, *Phys. Rev. B* **2008**, *77*, 214411.

[22] V. E. Demidov, M. P. Kostylev, K. Rott, P. Krzysteczko, G. Reiss, S. O. Demokritov, *Appl. Phys. Lett.* **2009**, *95*, 112509.

[23] J. P. Parekh, K. W. Chang, H. S. Tuan, *Circuits, Syst. Signal Process.* **1985**, *4*, 9.

[24] A. V. Chumak, A. A. Serga, M. B. Jungfleisch, R. Neb, D. A. Bozhko, V. S. Tiberkevich, B. Hillebrands, *Appl. Phys. Lett.* **2012**, *100*, 082405.

[25] M. B. Jungfleisch, A. V. Chumak, V. I. Vasyuchka, A. A. Serga, B. Obry, H. Schultheiss, P. A. Beck, A. D. Karenowska, E. Saitoh, B. Hillebrands, *Appl. Phys. Lett.* **2011**, *99*, 182512.

[26] Y. Tserkovnyak, A. Brataas, G. E. W. Bauer, *Phys. Rev. B* **2002**, *66*, 224403.

[27] E. Saitoh, M. Ueda, H. Miyajima, G. Tatara, *Appl. Phys. Lett.* **2006**, *88*, 182509.

[28] B. A. Kalinikos, *Sov. Phys. J.* **1981**, *24*, 718.

[29] P. H. Bryant, J. F. Smyth, S. Schultz, D. R. Fredkin, *Phys. Rev. B* **1993**, *47*, 11255.

[30] K. Y. Guslienko, R. W. Chantrell, A. N. Slavin, *Phys. Rev. B* **2003**, *68*, 024422.

[31] S. Chen, M. N. Afsar, *IEEE Trans. Magn.* **2007**, *43*, 2734.